CHAPTER III
EXPERIMENTAL

3.1 Material

Fine stone particles used in the fluidized bed were fine stones. Theirs properties are shown in Table 3.1. The particles were fluidized easily and the bubbles were generated slightly above the incipient fluidization velocity. The bed expansion was small and the bed collapsed rapidly when the gas supply was cut off. The rise velocities of the bubbles depended on bubble size and most bubbles traveled faster than the interstitial gas velocity, U_{mf}/ε_{mf}, so that gas tended to circulate within the bubble.

Table 3.1 Physical properties of particles.

Density	2.969 g/cm^3
Diameter	0.212-0.250 mm
Void fraction	0.4803
Minimum fluidizing velocity	5.127 cm/sec

3.2 Equipment

The schematic diagram and scale of the two-dimensional fluidized bed are shown in Figures 3.1 and 3.2. The system consisted of two sections: the distributor and the fluidized bed. The air (the continuous phase) was used as the fluidizing medium and flowed upward through the distributor. The solids were used batchwise, the particles remained in the bed all the time. The air flow rates were measured by a rotameter. The pressure tap was connected to a water manometer at the lower part of the column containing the particles for the measurement of the static pressure to estimate the minimum fluidizing velocity. The minimum fluidizing velocity was measured by using the graph of pressure drop against the air velocity. In this graph, two separated lines were drawn through the points of the fixed region that the pressure drop increased rapidly with increasing air velocity and the fluidized region that the pressure drop increased slightly with increasing air velocity. The point of intersection between these two lines was the minimum fluidizing velocity.

The column was a rectangular box made of transparent plastic, acrylic. The box was 15 cm in width, 60 cm in height, with a separation of 5 mm between the two large sides. At the bottom of the column a perforated plated distributor was used. Figure 3.2 shows the schematic diagram of the perforated plate distributor. The distributor was a rectangular plate, 15 cm in width, 5 mm in length, and 2 mm in thickness. The holes in the distributor were of two sizes. The one large size was 3.2 mm in diameter for the tube through which single air bubbles were injected. The twenty-eight small sizes for fluidizing the bed had a diameter of 0.69 mm. The total open area, the fraction of the total area occupied by the twenty-eight holes for fluidizing the particles, was 1.396%.

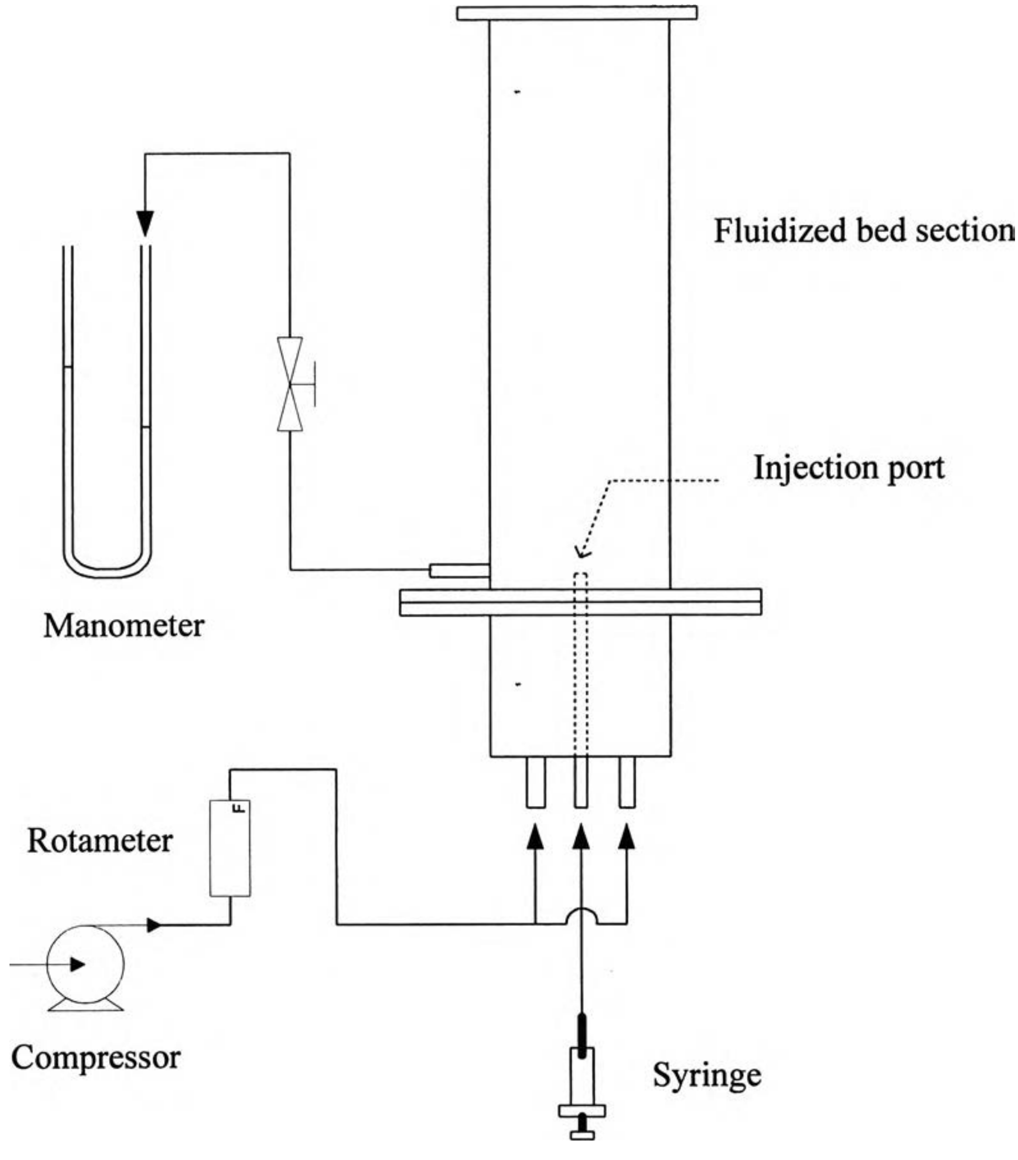

Figure 3.1 Schematic diagram of the two-dimensional fluidized bed.

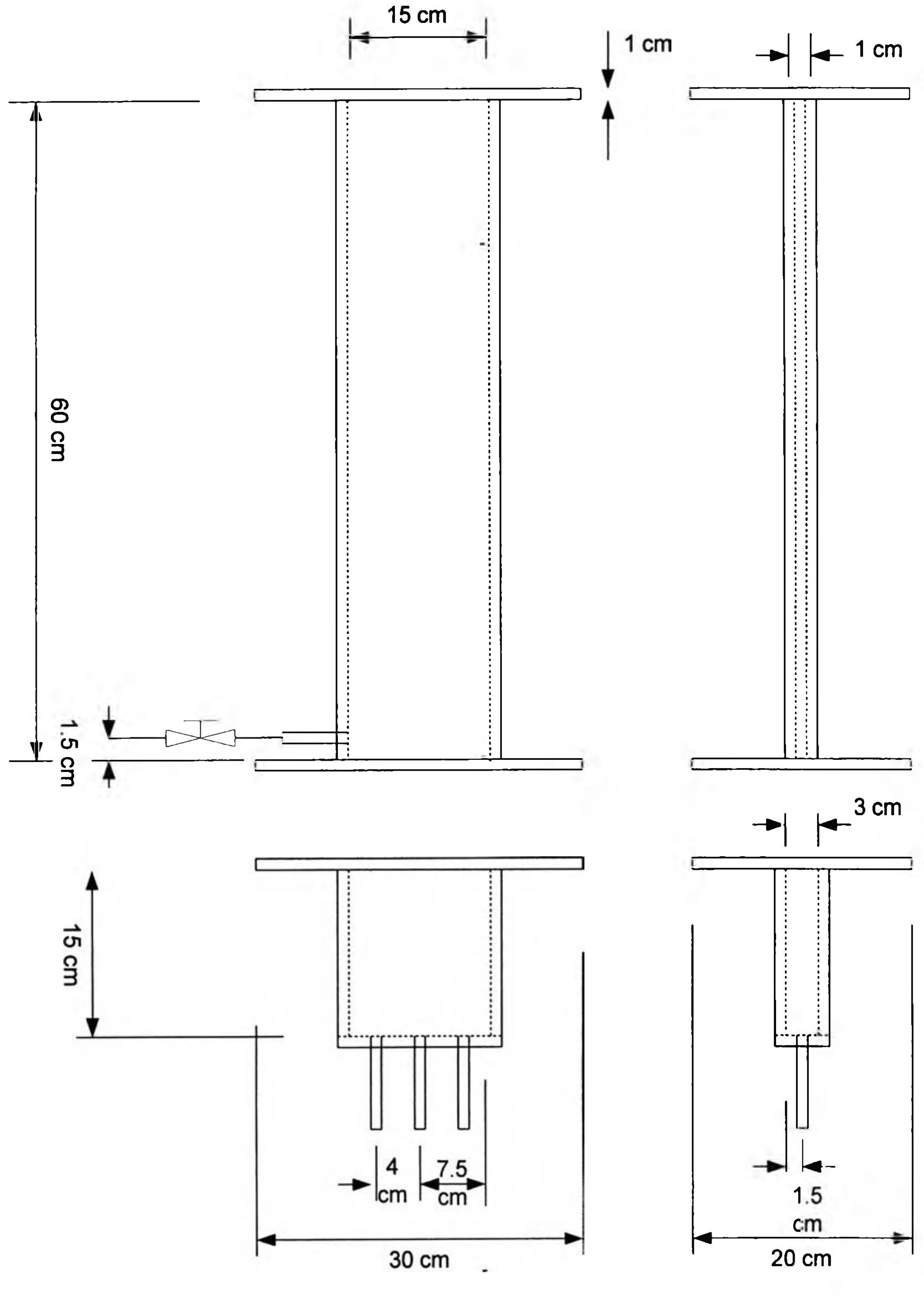

Figure 3.2 Scale of the two-dimensional fluidized bed.

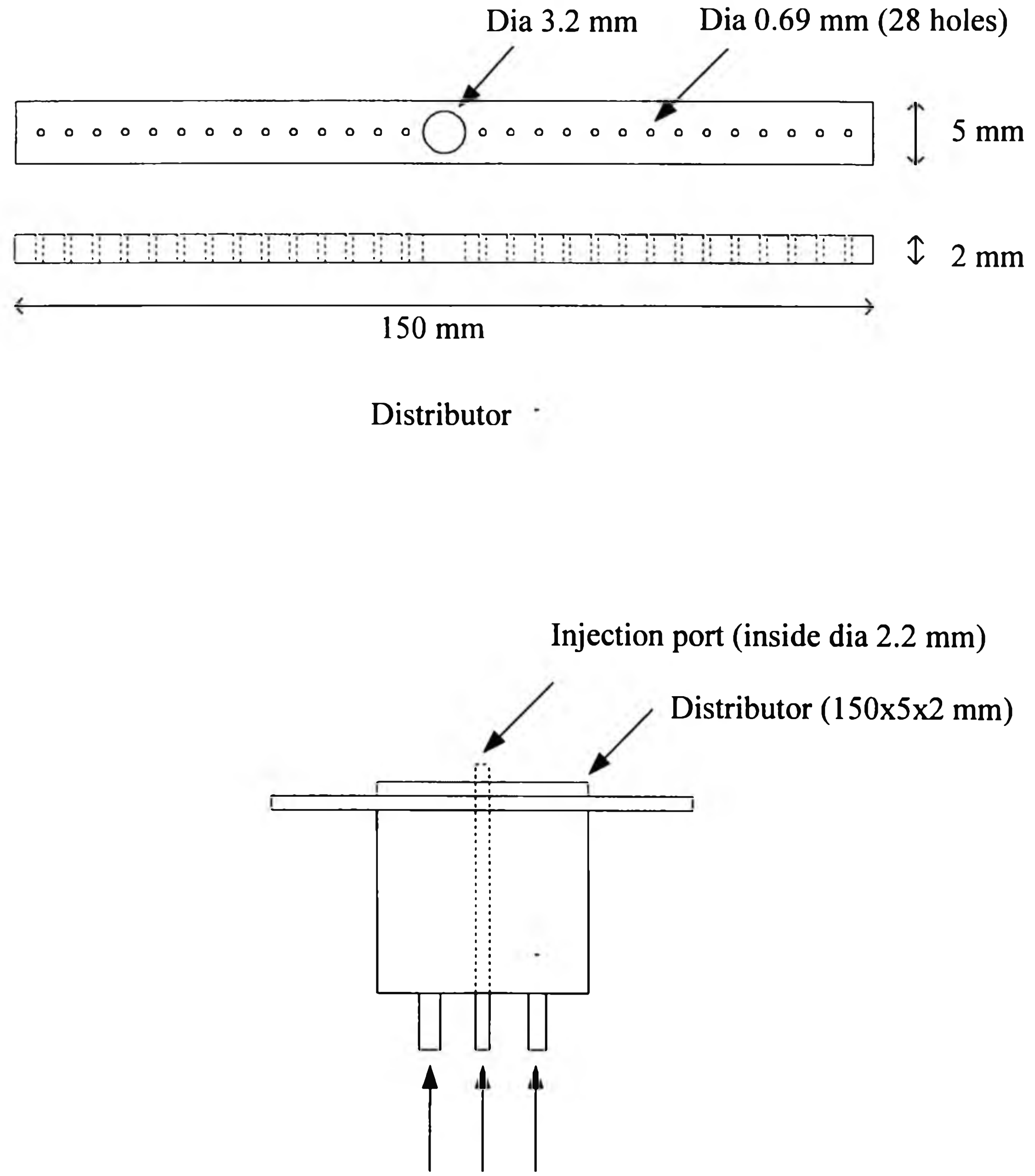

Figure 3.3 Schematic diagram of the perforated plate distributor.

3.3 Methodology

The movement of the bubbles in the fluidized bed was recorded by the video camera. The analog signal from the video cassette recorder was converted to a digital signal by the video capture card. The Windows Media Player program showed the movie at 25 frames/s. The time interval between frames was 0.04 s. At this rate the movie was played frame by frame, was captured into the picture by the Paint Shop program, and was calculated the surface area of the bubbles by the Adobe Photoshop program.

3.3.1 <u>The Rise Velocity of a Single Bubble</u>

To study the rise velocity of single bubbles in the stagnant fluid, the solids in the column were fluidized by air at the minimum fluidization rate. The syringe generated the bubbles rising through the bed shown in Figure 3.3. The sizes of the bubbles were varied by the volume of the air in the syringe. The effective bubble diameter was computed from the cross-sectional area of the bubble which was measured from the Adobe Photoshop program by changing the irregular shape of the bubble into the cylindrical shape that was the same area. The picture of a bubble was inserted to the Adobe Photoshop program for determining a number of pixels of the smallest dots in the computer screen comprising into the picture by Histogram mode. The rectangular paper that had exact area in the metric unit (square centimeter) was determined a number of pixels. Then, the pixels of bubble were compared with pixels of the rectangular paper to calculate the surface area of the bubble in the metric unit. The rise velocity was the space between bubbles divided by the time interval.

The rise velocities at the several bubble diameters were modeled with the rise velocity of bubbles in an infinite medium for deep inviscid liquid to predict the rise velocity and the deviation of the experiment results. In the experiment the fluidized bed was fluidized at the 2.5 l/min in the airflow rate or 5.56 cm/s in the air velocity.

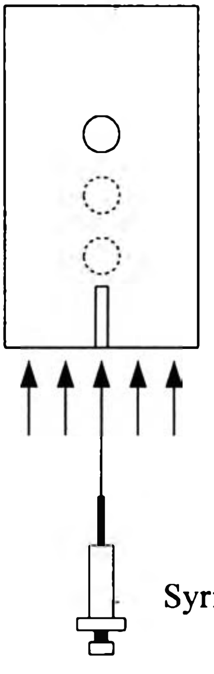

Figure 3.4 Mechanism of a single bubble in the fluidized bed.

3.3.2 The Volume of the Bubble Formed at an Orifice

The bubble was generated by the air whose flow rate corresponded to that need of incipient fluidization. Because the bubbles coalesced before they detached from the orifice, the air was fed directly from the syringe to the rotameter in order to measure the airflow rate and created the bubble. The volume of the bubble shown in Figure 3.4 was observed. The bubble volume at the various flow rates was modeled using the mass and momentum balances in order to estimate the bubble volume and the detachment time of the bubble.

The bubble volume was estimated from the picture of the bubble detaching from the orifice. The bubble volume of the cylindrical shape was the product of its cross-sectional area and the space between the parallel plates. To compute the volume, the Adobe Photoshop program was used to calculate the area when the bed was fluidized at 2.5 l/min.

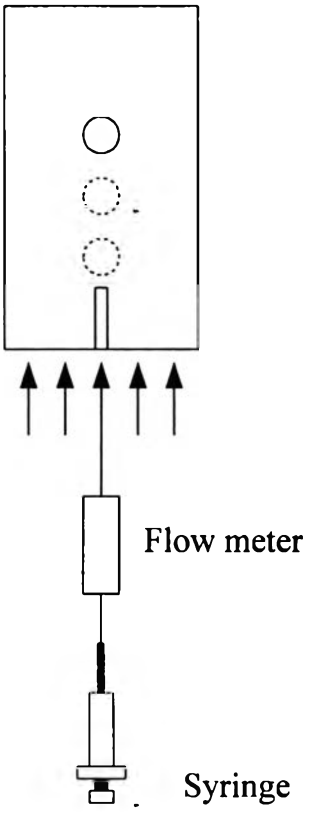

Figure 3.5 Mechanism of the bubble formation in the fluidized bed.

3.3.3 The Rise Velocity of a Continuous Swarm of Small Bubbles

Feeding the air to fluidize the bed above incipient fluidization, swarms of the bubbles were created as shown in Figure 3.5. The bed was full of the continuous bubbles and was expanded because of the presence of the bubbles. The bed heights at the various flow rates were measured for calculating the rise velocity and the size of the bubbles.

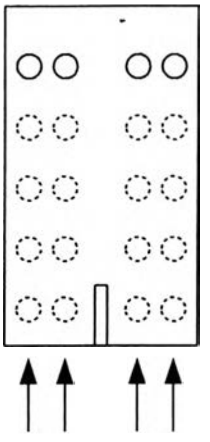

Figure 3.6 Mechanism of a continuous swarm of small bubbles in the fluidized bed.

3.4 Finite Element Program

The finite element program consists of FORTRAN source code with one main program and six subprograms. By assuming that the angular velocity of gas in the two-dimensional system shown in equation 3.1 was equal to zero or in an irrotational condition, the streamlines were calculated from in the partial differential equation shown in equation 3.2.

$$\omega = \frac{1}{2}\left(\frac{\partial v_y}{\partial x} - \frac{\partial v_x}{\partial y}\right) \quad (3.1)$$

$$\frac{\partial}{\partial x}k\frac{\partial \psi}{\partial x} + \frac{\partial}{\partial y}k\frac{\partial \psi}{\partial y} = 0 \quad (3.2)$$

To solve the problem, the area of the system was divided into elements. The initial variables for computation, such as the number of the nodes and elements, the element coordinates, nodal numbers of each element, and the boundary conditions were added in the 'Input.dat' file of the FORTRAN PowerStation 4.0 program for determining the values of the air streamlines in the main program. The ELEMENT subprogram as shown in Figure 3.6 calculated the area of each element, checked the elemental connections, and computed the coefficients in the element equations. To create the system of equations, the MATRIX subprogram was called from the main program and transferred the system of equations to the BOUNDARY subprogram for setting the boundary conditions. The Gauss elimination method for computing the streamlines of each node was called from the GAUSS subprogram. During the computation, the GAUSS subprogram called the PIVOT subprogram for rearranging the system of equations and the SCAL subprogram for reducing the scale of the coefficients in system of equations. The results of air streamlines were computed from the GAUSS subprogram and were displayed in the 'Output.dat' file of Fortran PowerStation 4.0 program.

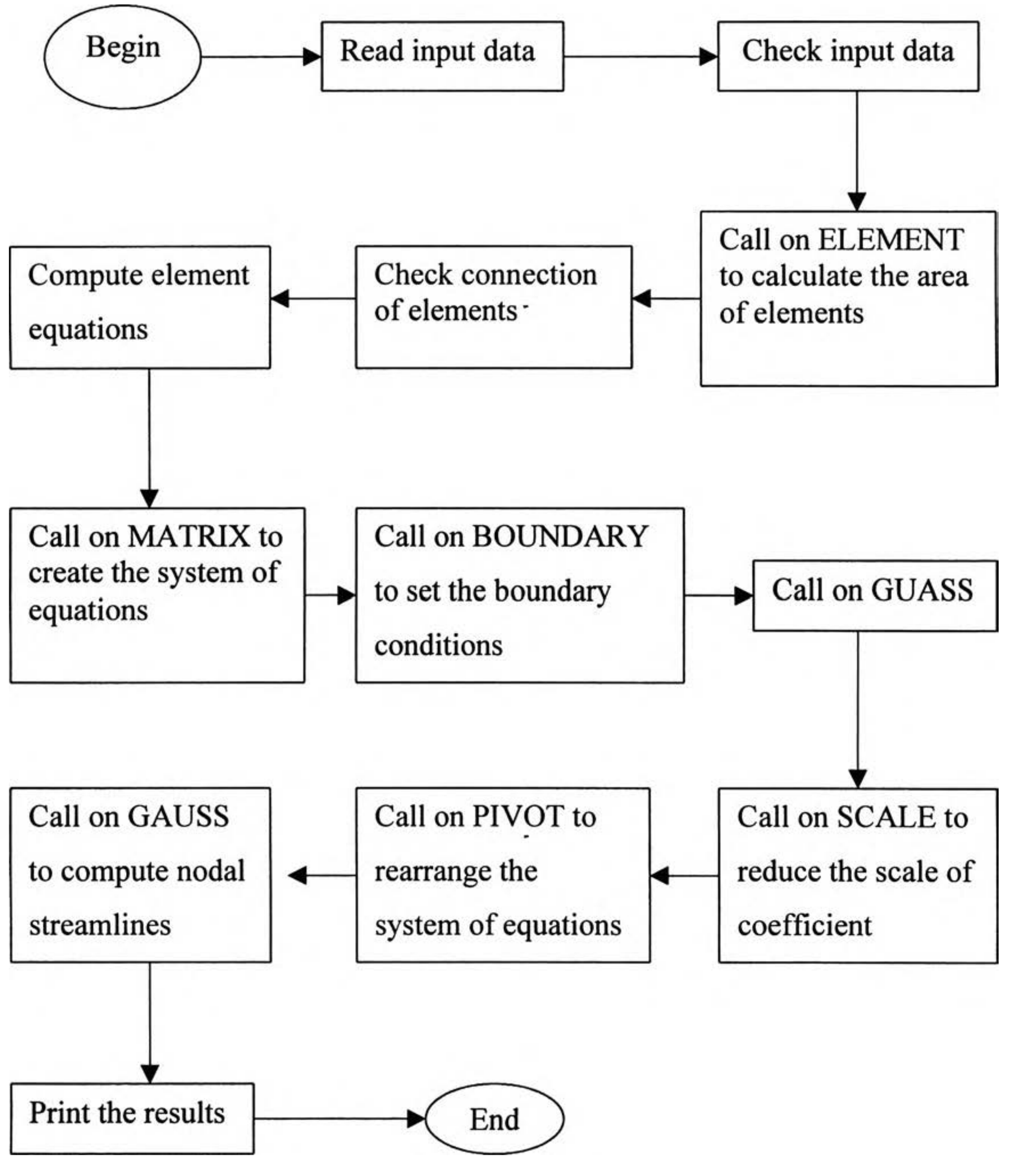

Figure 3.7 A general flow diagram for the finite element program.